Measurement of up-conversion energy-transfer probabilities in $Ho:Y_3Al_5O_{12}$ and $Tm:Y_3Al_5O_{12}$

L. B. Shaw, R. S. F. Chang, and N. Djeu
Department of Physics, University of South Florida, Tampa, Florida 33620-5700
(Received 26 January 1994; revised manuscript received 9 May 1994)

The probabilities for up-conversion involving two nearest-neighbor $Ho^{3+}(^5I_7)$ ions and $Tm^{3+}(^3F_4)$ ions in $Y_3Al_5O_{12}$ have been determined. The final states are $^5I_5$ and $^5I_6$ for Ho^{3+} and $^3H_4$ and $^3H_5$ for Tm^{3+}. A rate-equation model has been used to obtain an expression for the concentration dependence of the up-conversion-rate constant in the migration-limited regime. We have also measured the reverse cross-relaxation probabilities for two of the processes with $Ho^{3+}(^5I_5)$ and $Tm^{3+}(^3H_4)$ as donors. The results fit well to the energy-gap law for phonon-assisted energy transfer. They also show evidence that there may be a correlation between the deviations from the energy-gap law for opposite processes.

I. INTRODUCTION

Up-conversion involving excited ionic species in crystals has been a subject of considerable interest for over two decades now.[1] For the most part the experimental investigations in this area have been of a qualitative nature. The growing importance of up-conversion-pumped lasers, in the strict sense[2–4] as well as the broad sense,[5–8] and high-storage-density solid-state lasers[9–12] in recent years has provided an impetus to seek a more quantitative understanding of this type of process. To this end, we embarked on a systematic experimental study of up-conversion involving the first excited state in $Ho:Y_3Al_5O_{12}$ and $Tm:Y_3Al_5O_{12}$. The two ions chosen have similar simple energy-level structures for the lowest-lying states and therefore provide the opportunity for a comparative examination of the data.

In our experiments the up-conversion processes were studied by direct pumping of the metastable first excited state with short laser pulses. The subsequent emissions from higher-lying states as well as the pumped state were then analyzed in the quasi-steady-state regime. This was done at a number of dopant concentrations for each of the two rare-earth ions. Rate equations taking into account all significant energy transfer and relaxation pathways were employed to obtain the state-specific up-conversion rate constants. This procedure necessitated the measurement of a number of multiphonon and cross relaxation rates first. This was accomplished by direct excitation of the states involved with pulsed lasers at the appropriate wavelengths.

The theoretical tools needed to describe an elementary up-conversion process, i.e., the interaction of two initially excited ions at a fixed distance resulting in an upward nonradiative transition for one of them and a downward one for the other, are the same as those for the opposite cross relaxation process. These theories are reasonably well developed, and have been supported by experiments in some instances.[13–15] However, to our knowledge no comprehensive description of up-conversion taking into account the possibility of excitation migration has been offered till now. Models for migration-limited cross relaxation[16,17] are not applicable here, since in up-conversion both donor and acceptor ions must be excited. In this paper we propose a model for migration-limited up-conversion based on a rate equation approach to the excitation migration process. Our model fits well the experimentally determined up-conversion rate constants. From such fits nonradiative transition probabilities for up-conversion and excitation migration were inferred.

II. MIGRATION-LIMITED UP-CONVERSION MODEL

We start by presenting a microscopic model of the up-conversion process. In this model it is assumed that up-conversion can take place only between nearest-neighbor ions. It will be argued later that this is a good assumption except at very low dopant concentrations. We consider the collection of dopant ions that occupy nearest-neighbor sites in the host crystal. These nearest-neighbor (NN) pairs can contain no excited ion, one excited ion, or two excited ions. For the experimental cases of interest here we will be concerned with two like excited ions. Each pair is imagined to exchange excitation with the surrounding at a characteristic rate. The task is then to find the density of NN pairs in which both ions are excited.

Let the densities of NN pairs with no excited ion, one excited ion, and two excited ions be denoted by N_{p0}, N_{p1}, and N_{p2}, respectively. We assume that the ion which is promoted to a higher excited state as a result of the up-conversion process relaxes instantaneously back to its original state. Then $N_{p0}+N_{p1}+N_{p2}=N_p$, the total density of NN pairs, and all ions in the system are either in the ground state or in the excited state which undergoes up-conversion. Let the densities of excited and unexcited ions be N_e and N_g, so that $N_e+N_g=N$, where N is the total density of dopant ions in the crystal. We assume that the rate constant for excitation transfer is independent of whether it is from an excited ion in a NN pair to the surrounding or vice versa and is also independent of the degree of excitation of a NN pair. Then one may write the following rate equations:

$$\frac{dN_{p0}}{dt}=-2kN_eN_{p0}+(kN_g+A)N_{p1}\ , \tag{1}$$

$$\frac{dN_{p1}}{dt}=2kN_eN_{p0}-(kN_g+A+kN_e)N_{p1} +(2kN_g+2A+U)N_{p2}\ , \tag{2}$$

$$\frac{dN_{p2}}{dt}=kN_eN_{p1}-(2kN_g+2A+U)N_{p2}\ , \tag{3}$$

where A is the radiative rate of the metastable state, k is the phenomenological rate constant for excitation transfer between the ion pairs and the surrounding, and U is the up-conversion probability per unit time for a doubly excited NN pair. Note that while the relative excitations of the NN pairs and the surrounding may not be equilibrated, the excitation within the surrounding itself is assumed to be always equilibrated in this model. Thus, for each ion in the NN pair the surrounding can be represented by a single ion, located at a characteristic distance R_c away, whose probability of being in the excited state or the ground state bears the ratio N_e/N_g. If a dipole-dipole interaction is assumed, one can find the phenomenological rate constant k from

$$kN=\frac{C_m}{R_c^6}\ , \tag{4}$$

where C_m is the microparameter for excitation migration.[18] For a purely statistical distribution of the ions and low fractional concentration of NN pairs, R_c can be construed to be the average distance between closest ions given by[19]

$$R_a=\left[\frac{1}{N}\right]^{1/3}\ . \tag{5}$$

Then one obtains

$$k=C_mN\ . \tag{6}$$

In steady state, Eqs. (1)–(3) can be solved subject to the condition $N_{p0}+N_{p1}+N_{p2}=N_p$ to give

$$N_{p2}=\frac{2kN_e^2N_p}{2k(N_e+N_g+A/k)^2+(2N_e+N_g+A/k)U}\ . \tag{7}$$

For $N_p \ll N$, and N_e and $A/k \ll N_g$, one may write

$$N_{p2}=\frac{N_e^2N_p}{N(N+U/2k)}\ . \tag{8}$$

We note that this steady-state solution would still be valid if the time derivatives dN_{pi}/dt are small compared to the terms containing the respective N_{pi} in Eqs. (2) and (3).

For a purely statistical distribution of dopant ions among the available sites, the concentration of ions with n nearest neighbors is given by[20]

$$c_n=\frac{n_0!}{n!(n_0-n)!}c^{n+1}(1-c)^{n_0-n}\ , \tag{9}$$

where c is the total dopant concentration and n_0 is the maximum number of nearest neighbors possible (the number of sites in the first coordination sphere). If we take the view that an ion with n nearest neighbors is equivalent to n NN pairs, then

$$\sum_{n=1}^{n_0}nc_n=n_0c^2\ , \tag{10}$$

together with Eqs. (6) and (8), lead to

$$N_{p2}=\frac{c^2}{c^2+c_0^2}\frac{2N_e^2}{N_s}\ , \tag{11}$$

where

$$c_0^2=\frac{U}{2C_mN_s^2}\ , \tag{11'}$$

and N_s is the dopant ion density for $c=1$. In writing Eq. (11) we have made use of $N_p=n_0c^2N_s/2$ and $n_0=4$ for $Y_3Al_5O_{12}$.[21] The volumetric up-conversion rate then is simply UN_{p2}. In the limit that $c \ll 1$, Eq. (11) is obtained without any assumption about the role of clusters with more than two ions.

III. MACROSCOPIC RATE EQUATIONS

Experimentally the extent of up-conversion is inferred from emission from the up-converted states. Therefore, in order to interpret the data one must write down a set of rate equations relating the densities of the up-converted states to the density of the up-converting state. The densities in these macroscopic rate equations are overall densities without regard to the immediate environment of the ionic species. As we will show below, the explicit inclusion of the up-converted states in the macroscopic rate equations does not necessarily contradict our assumption in the preceding section that they may be disregarded in the rate equations for the NN pairs.

The lowest four levels in Ho:$Y_3Al_5O_{12}$ and Tm:$Y_3Al_5O_{12}$ are shown schematically in Fig. 1. In the case of Ho:$Y_3Al_5O_{12}$, levels 0, 1, 2, and 3 are $^5I_8$, $^5I_7$, $^5I_6$, and $^5I_5$ with energies of 0 cm^{-1}, 5228 cm^{-1}, 8733 cm^{-1}, and 11 320 cm^{-1}, respectively (for the lowest Stark level in each multiplet). For Tm:$Y_3Al_5O_{12}$ they are $^3H_6$, $^3F_4$, $^3H_5$, and $^3H_4$ situated at 0 cm^{-1}, 5556 cm^{-1}, 8339 cm^{-1}, and 12 607 cm^{-1}. With reference to the state-specific processes indicated in Fig. 1, we obtain the following rate equations:

$$\frac{dN_1}{dt}=-2(U_{12}+U_{13})N_1^2-A_{10}N_1 +(2C_{21}N_0+M_{21}+A_{21})N_2+(2C_{31}N_0+A_{31})N_3\ , \tag{12}$$

$$\frac{dN_2}{dt}=U_{12}N_1^2-(C_{21}N_0+M_{21}+A_{21}+A_{20})N_2 +(M_{32}+A_{32})N_3\ , \tag{13}$$

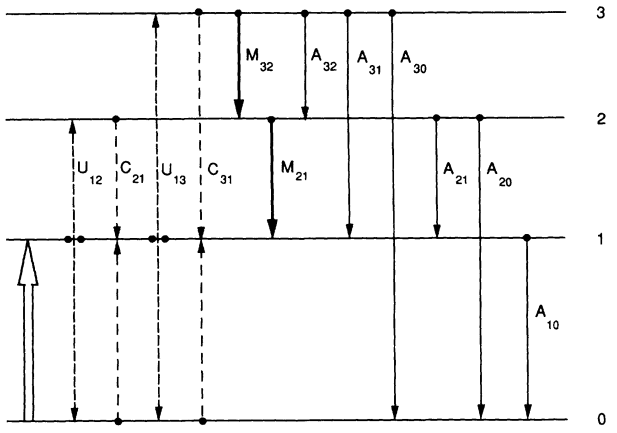

FIG. 1. Schematic of the four lowest-lying energy levels in Ho^{3+} or Tm^{3+} showing the radiative and nonradiative processes used in our model. Each level represents a multiplet composed of a number of Stark sublevels.

$$\frac{dN_3}{dt}=U_{13}N_1^2-(C_{31}N_0+M_{32}+A_{32}+A_{31}+A_{30})N_3 \ , \tag{14}$$

where N_i is the density of level i, U_{ij} the up-conversion-rate constant from i to j, C_{ij} the cross-relaxation rate constant from i to j, M_{ij} the multiphonon relaxation rate from i to j, and A_{ij} the radiative decay rate from i to j. In these equations all the cross-relaxation processes are assumed to occur with superfast migration, while the up-conversion processes are allowed to be migration limited by making the U_{ij}'s concentration dependent quantities.

In steady state these equations lead to

$$N_3=\frac{U_{13}}{C_{31}N_0+Q_3}N_1^2 \tag{15}$$

and

$$N_2=\frac{1}{C_{21}N_0+Q_2}\left[U_{12}+\frac{M_{32}+A_{32}}{C_{31}N_0+Q_3}U_{13}\right]N_1^2 \ , \tag{16}$$

where $Q_2=M_{21}+A_{21}+A_{20}$ and $Q_3=M_{32}+A_{32}+A_{31}+A_{30}$. The quadratic dependence of N_2 and N_3 on N_1 is expected, given the assumed quadratic nature of the up-conversion process. As before, these results are valid even in the quasi-steady-state regime, where dN_2/dt and dN_3/dt are small compared with the terms containing N_2 and N_3 in Eqs. (13) and (14), respectively. Note that the determination of U_{13} and U_{12} requires not only knowledge of the radiative, multiphonon, and cross-relaxation rates, but also the absolute densities of the levels involved.

We must now reconcile the macroscopic rate equations with those for the NN pairs. In the former we allowed for the possibility of up-conversion to two states, while in the latter to only one. This would not cause any difficulty if up-conversion to the second state is either negligible or followed immediately by the reverse cross relaxation process. As will be seen later, one of these conditions is satisfied for up-conversion to $^5I_5$ in $Ho:Y_3Al_5O_{12}$ and the other condition for up-conversion to $^3H_4$ in $Tm:Y_3Al_5O_{12}$. Also, one is justified not to take into account in the rate equations for the NN pairs the up-converted states if the total density in each of the up-converted states is small compared to that of the up-converting state. This condition again is always satisfied under our experimental conditions. Thus, as far as the interpretation of our data is concerned there is no conflict between the two sets of rate equations. Combining the two views and recognizing the equivalence of N_e and N_1, we find the relationship

$$U_{12}=\frac{c^2}{c^2+c_0^2}\frac{2U}{N_s} \ , \tag{17}$$

where U is the probability of up-conversion per unit time for a doubly excited NN pair to give one ion in 2 and one ion in 0. If we let U' be the corresponding probability per unit time for up-conversion to 3, it is clear from our model that it must be related to U_{13} by

$$U_{13}=\frac{c^2}{c^2+c_0^2}\frac{2U'}{N_s} \ , \tag{18}$$

where c_0 is the same as that in Eq. (17). Thus the elementary up-conversion transition probabilities can be found from the macroscopic up-conversion rate constants. Note that according to Eq. (17) the average rate of up-conversion to 2 for a single excited ion is given by $U_{12}N_1=n_0Uc_e/2$, where c_e is the concentration of excited ions, in the limit of superfast migration ($c \gg c_0$).

IV. EXPERIMENTAL DETAILS

The crystals used in our measurements were grown by the laser heated pedestal growth technique.[22] They typically measured just under 1 mm in diameter and several hundred microns in thickness. The small diameter was necessitated by the desire to maximize excitation density with the available laser energies, and the small thickness to ensure axial uniformity of excitation to less than 10% variation as well as to minimize the effect of edge diffraction. The dopant concentrations were determined by absorption spectroscopy and were found to be close to the expected concentrations from the compositions of the starting mixtures. The samples were polished to an optical flatness on both ends.

The various laser sources were all driven by a 1-J, 10-nsec Nd:YAG laser or its second harmonic. They included a H_2 vibrational Raman laser at 1.91 μm for the pumping of the $^5I_7$ level in Ho^{3+}, a HD vibrational Raman laser at 1.73 μm for the pumping of the $^3F_4$ level in Tm^{3+}, a H_2 rotational Raman laser at 1.14 μm for the excitation of the $^5I_6$ level in Ho^{3+}, and a Ti:sapphire laser operating at 872 nm, 767 nm, and Raman shifted to 1.2 μm for the excitation of $Ho^{3+}(^5I_5)$, $Tm^{3+}(^3H_4)$, and $Tm^{3+}(^3H_5)$, respectively. The spatial profile of the beam was found to be smooth for each of the laser sources. Only the central portion of each of the beams was used to ensure uniformity of excitation to $\pm 10\%$ across the diameter of the crystal.

The evolution of the various excited-state densities in time was monitored via their fluorescence, which was collected by a lens and detected after passage through appropriate filters and/or a $\frac{1}{8}$-m monochromator. For the multiphonon and cross relaxation measurements only the shapes of the time-dependent fluoresence signals were needed. For the up-conversion measurements the absolute densities of the states involved had to be determined. For the up-converting state the initial signal level corresponded directly to the density calculated from the measured absorbed energy and the known volume of the crystal. For the up-converted states the fluorescence had to be calibrated against that obtained from the direct excitation of the same state with a known laser energy and using an identical geometry. All the measurements were made at room temperature.

V. Ho:$Y_3Al_5O_{12}$ RESULTS

For the measurement of multiphonon and cross relaxation rates of $Ho^{3+}(^5I_6)$ the 1.14-μm source was used. The time-dependent emissions from 3%-, 5%-, and 10%-doped samples were monitored near 1.2 μm. In each case the decay was found to be purely exponential. Within experimental errors the decay rate was the same for all three concentrations. From these results we obtain a multiphonon rate of $M_{21}(Ho^{3+})=(2.2\pm0.1)\times10^4$ sec^{-1} and an upper bound for the cross relaxation rate constant $C_{21}(Ho^{3+})<2\times10^{-18}$ $cm^3\,sec^{-1}$.

Similar measurements were made on the relaxation of the $^5I_5$ state using the pulsed Ti:sapphire laser operating at 872 nm. The decay signals can again be fitted very well to pure exponentials for all the concentrations studied. The decay rates for the different Ho^{3+} concentrations are plotted in Fig. 2. From the best straight-line fit the cross relaxation rate constant and the multiphonon relaxation rate are found from the slope and the intercept to be $C_{31}(Ho^{3+})=(7.8\pm0.8)\times10^{-16}$ $cm^3\,sec^{-1}$ and $M_{32}(Ho^{3+})=(7.6\pm0.8)\times10^5$ sec^{-1}.

For the up-conversion measurements more than 20 mJ at 1.91 was available from the H_2 Raman laser. However, only a few millijoules near the center of the beam were used to ensure radial excitation uniformity. The absolute densities of the various states were determined using the procedure outlined in the preceding section. Thus, for example, the $^5I_5$ density was obtained by comparing the fluorescence signal near 900 nm from up-conversion with the initial signal at the same wavelength following direct excitation by a known amount of laser energy at 872 nm under identical detection arrangements. The signals from $^5I_7$ and either $^5I_5$ or $^5I_6$ produced by the same incident 1.91-μm beam energy were analyzed in pairs. The density of $^5I_5$ or $^5I_6$ at a given time after the excitation pulse is plotted against the density of $^5I_7$ after the same time delay. Such a plot for $^5I_6$ density vs $^5I_7$ density for a 2% Ho:$Y_3Al_5O_{12}$ sample is shown in Fig. 3(a). The plot includes the results from several pairs for different incident 1.91-μm beam energies. The range of time delay used for each set is from 200 μsec to 10 msec. It is seen that a good fit to a quadratic dependence of N_2 on N_1 is ob-

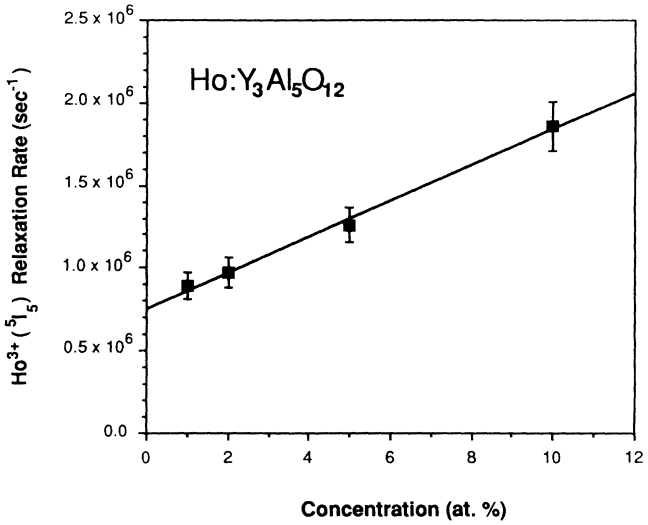

FIG. 2. Total exponential decay rate of Ho^{3+} ($^5I_5$) vs Ho^{3+} concentration.

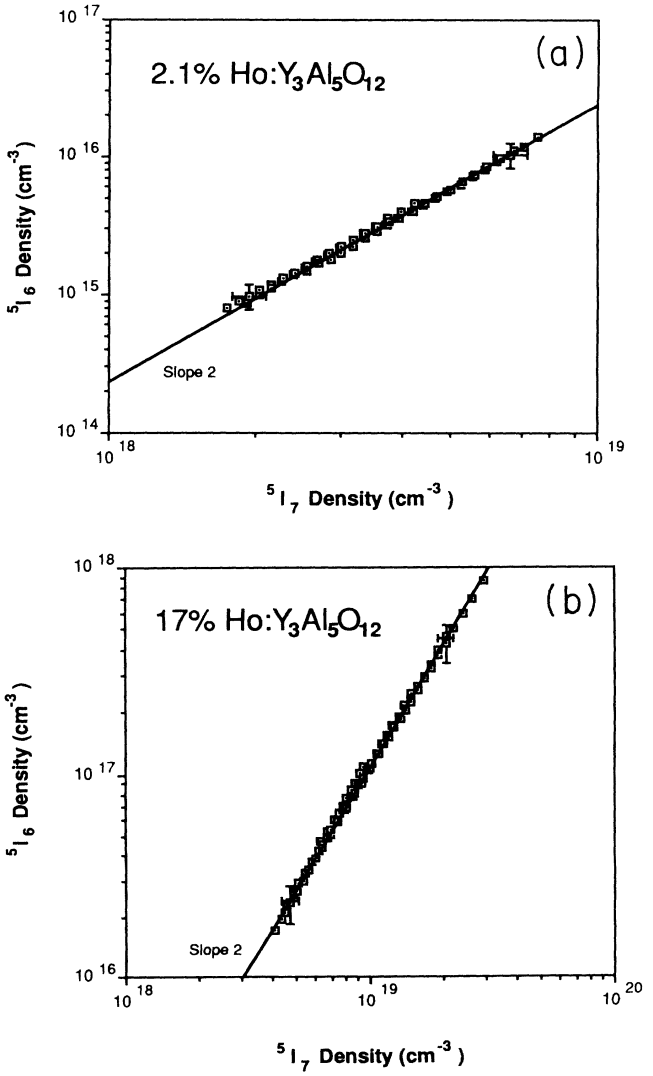

FIG. 3. Quasi-steady-state density of Ho^{3+} ($^5I_6$) plotted against that of Ho^{3+} ($^5I_7$) for (a) 2.1% Ho:$Y_3Al_5O_{12}$ and (b) 17% Ho:$Y_3Al_5O_{12}$.

tained. A similar plot for a 17% sample is shown in Fig. 3(b).

When the procedure is applied to N_3 vs N_1, the same result is obtained at low concentrations, as shown in Fig. 4(a). However, at higher concentrations the data can no longer be fitted to a single slope 2 line. A good fit can only be obtained by using a sum of the slope 2 and slope 3 lines. This is shown in Fig. 4(b) for the 17% sample. We interpret this as an indication that at high Ho^{3+} concentrations and high $^5I_7$ densities a three-ion up-conversion process begins to play a role.[23,24] Such a process would likely involve the excitation of one of the ions to the $^5I_4$ state and the deexcitation of the other two to the ground state. The $^5I_4$ state then rapidly decays to $^5I_5$, contributing to the fluorescence from the latter.

The up-conversion-rate constants U_{13} and U_{12} for each dopant concentration were calculated using Eqs. (15) and (16). Except for A_{10}, which was measured, the radiative rates needed were calculated under the Judd-Ofelt approximation,[25,26] with the necessary reduced matrix elements and intensity parameters taken from tables.[27] The results for up-conversion to $^5I_5$ are shown in Fig. 5. For the higher concentrations, U_{13} is derived from the slope-2 part of the N_3-vs-N_1 data. The concentration dependence of U_{13} was then fitted to Eq. (18). The points for the two lowest concentrations were not used in the fit, as the up-conversion model is believed to be less accurate for the lower concentrations. This follows because interactions between next-nearest-neighbor pairs become relatively more important at low concentrations, and they are not included in our model. (See further discussions in the final section.) The best fit was obtained for $U'=(1.0\pm0.3)\times10^4\ \mathrm{sec}^{-1}$ and $c_0=0.065$.

Once U_{13} was known U_{12} could be determined with the use of Eq. (16). The results are shown as squares in Fig. 6. The best fit to Eq. (17), leaving out the two

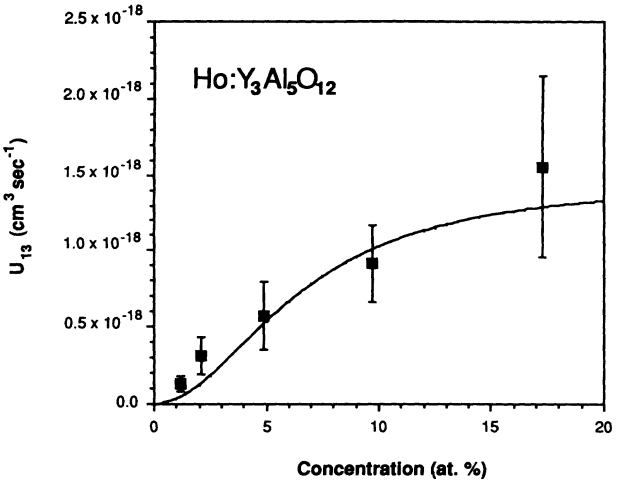

FIG. 5. Measured rate constants for up-conversion from Ho^{3+} ($^5I_7$) to Ho^{3+} ($^5I_5$) for different Ho^{3+} concentrations and their best fit to the model.

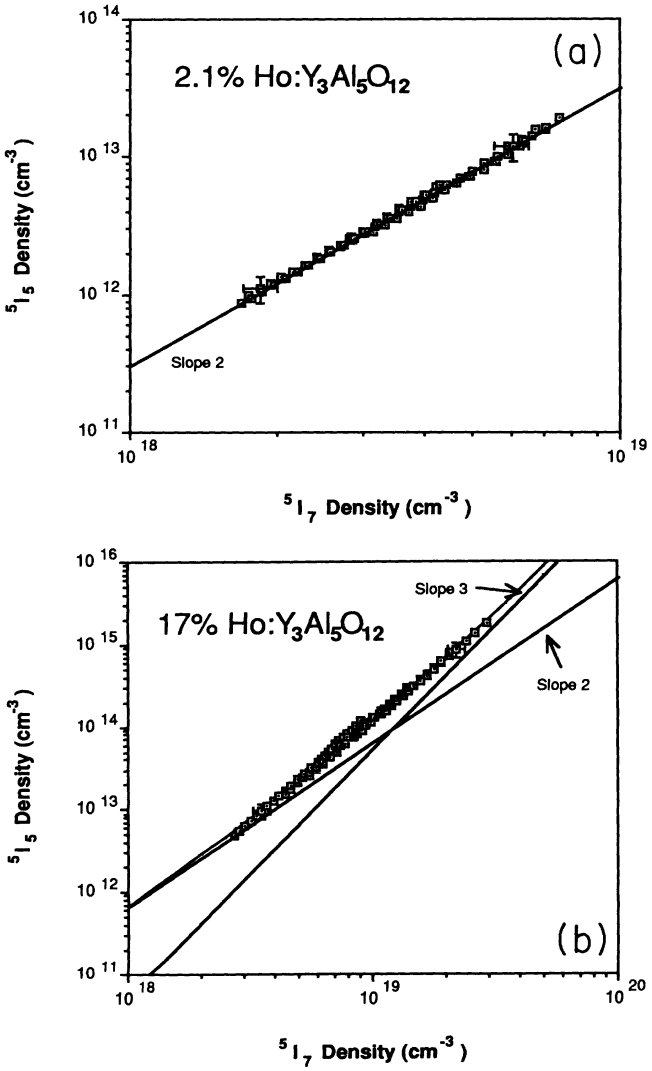

FIG. 4. Quasi-steady-state density of Ho^{3+} ($^5I_5$) plotted against that of Ho^{3+} ($^5I_7$) for (a) 2.1% $Ho:Y_3Al_5O_{12}$ and (b) 17% $Ho:Y_3Al_5O_{12}$.

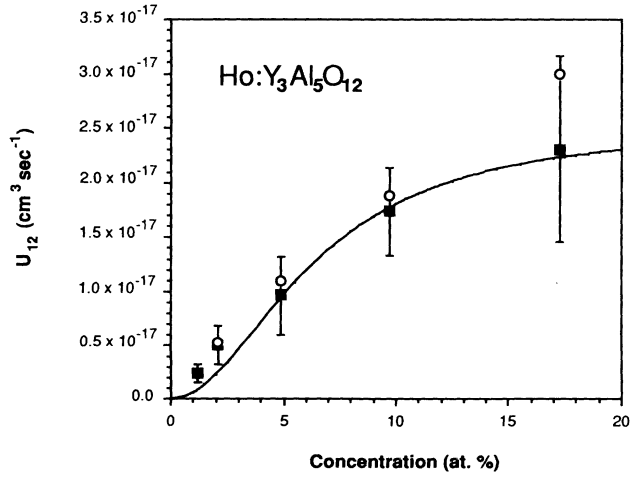

FIG. 6. Measured rate constants for up-conversion from Ho^{3+} ($^5I_7$) to Ho^{3+} ($^5I_6$) for different Ho^{3+} concentrations and their best fit to the model.

lowest concentration points, yielded $U=(1.7\pm0.4)\times10^5$ $\sec^{-1}$ and $c_0=0.064$. The agreement between the two values for c_0 found from the concentration dependences of U_{13} and U_{12} is better than we have reason to expect, given the relatively large error bars for the data points. Nevertheless, it gives an additional measure of confidence in the validity of our data. The up-conversion rate constant U_{12} can be obtained from the decay curve of N_1 alone under the assumptions that $A_{3i}\ll C_{31}N_0, M_{32}$ and $A_{2i}, C_{21}N_0 \ll M_{21}$. Then one finds

$$N_1(t)=\frac{A_{10}N_1(0)}{(U_{12}+U'_{13})[\exp(A_{10}t)-1]N_1(0)+A_{10}\exp(A_{10}t)}\ , \tag{19}$$

where

$$U'_{13}=\frac{M_{32}U_{13}}{C_{31}N_0+Q_3}\ . \tag{19'}$$

A representative fit of the decay curve of $^5I_7$ to Eq. (19) for a 4.7% sample is shown in Fig. 7. The up-conversion rate constants U_{12} obtained in this way are shown as circles in Fig. 6. It is seen that the agreement between the values found using the two different procedures is quite satisfactory.[28]

It remains to be shown that the quasi-steady state approximations made in the solutions of the macroscopic rate equations as well as those for the NN pairs are reasonable. The values of dN_2/dt and dN_3/dt can be found directly from the slopes of the experimental decay curves for N_2 and N_3. For the range of time delays for which the data in Figs. 3 and 4 were taken they never exceed 10% of the terms containing N_2 and N_3 in Eqs. (13) and (14), respectively. Therefore, the use of Eqs. (15) and (16) is justified. To check the validity of the steady-state assumption in the solution of Eqs. (1)–(3), the differential equations were solved numerically using the rates determined above and densities appropriate to our experimental conditions. It was found that dN_{p1}/dt and dN_{p2}/dt amount to less than 1% of the terms containing N_{p1} and N_{p2} in Eqs. (2) and (3), respectively, after the first 50 μsec for all samples except the 1% crystal. In the latter case, dN_{p1}/dt remained at approximately 10% of $(kN_g+A+kN_e)N_{p1}$ after the first 50 μsec. These results justify the use of Eq. (8). Furthermore, since U_{13} is only 6% of U_{12}, the neglect of up-conversion to N_3 in Eqs. (1)–(3) is also justified.

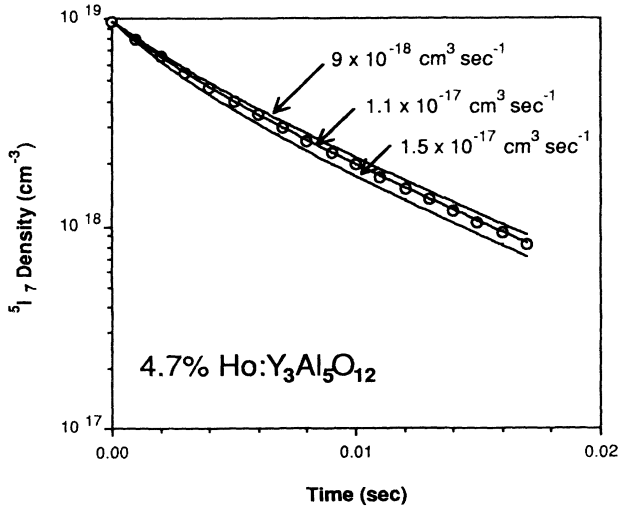

FIG. 7. Decay of Ho^{3+} ($^5I_7$) for a 4.7% Ho:$Y_3Al_5O_{12}$ sample when up-conversion loss is significant. Curves drawn according to Eq. (19) are shown for three different values of $U_{12}+U'_{13}$.

VI. Tm:$Y_3Al_5O_{12}$ RESULTS

Relaxation of the $^3H_4$ level of Tm^{3+} was studied with excitation at 767 nm. Only the initial portion of the decay curve was found to be exponential, indicating that its cross relaxation is migration limited.[17] The early part of the signal is associated mainly with Tm^{3+} ($^3H_4$) ions with nearest-neighbor Tm^{3+} ground-state ions. The trailing portion has $\exp(-\gamma\sqrt{t}\,)$ dependence and is due to Tm^{3+} ($^3H_4$) ions whose closest neighbors are not nearest neighbors (Förster decay). Such a bimodal decay for an 8% sample is shown in Fig. 8(a). For higher concentrations the exponential part becomes more and more dominant, as illustrated by the decay signal from a 17% sample shown in Fig. 8(b). The decay rates of the exponential portions are plotted against the concentrations of the samples in Fig. 9. The straight line is the best fit going through the calculated total rate of radiative and multiphonon relaxation for Tm^{3+} ($^3H_4$),[29] which on the scale of Fig. 9 is essentially zero. The C_{cr} on the vertical axis in Fig. 9 is the microparameter for the cross relaxation process and the summation is over all possible Tm^{3+} sites in the $Y_3Al_5O_{12}$ lattice. Using the known R_i's and their coordination numbers,[30] we find from the slope of the line $C_{cr}=(1.6\pm0.4)\times10^{-38}$ $cm^6\,sec^{-1}$. The probability for cross relaxation between NN Tm^{3+} ions is then $W(R_0)=C_{cr}/R_0^6=(6.4\pm1.5)\times10^6$ sec^{-1}. One can also determine C_{cr} from the trailing portions of the decay curves. Using the expression for γ given in Ref. 17, we find with this latter procedure a C_{cr} which is about 20% smaller than the one just given.

An attempt was made to study the decay kinetics of Tm^{3+} ($^3H_5$) by excitation at 1.2 μm. However, our detection system was not sensitive enough to give us a signal for any of the dopant concentrations. This is not surprising, since the calculated quantum efficiency for Tm^{3+}($^3H_5$) is only 3×10^{-3}.[29] Given the large multipho-

non relaxation rate of Tm^{3+} ($^3H_5$) and the large energy difference between $^3H_5 \rightarrow {}^3F_4$ and $^3H_6 \rightarrow {}^3F_4$, it is reasonable to assume that $C_{21}N_0 \ll M_{21}$.

Since the up-converted fluorescence from Tm^{3+} ($^3H_5$) was not detectable, we had to resort to the fitting of the Tm^{3+} ($^3F_4$) decay curve according to Eq. (19) to extract U_{12}. Even the latter approach was limited to a small concentration range of between 8% and 13% only. At lower concentrations, for the 1.73-μm pump energy available there was insufficient absorption to produce an observable up-conversion effect. At higher concentrations, there was significant shortening of the lifetime of the $^3F_4$ state, presumably due to impurity quenching,[31] and it was again not possible to extract U_{12}. The best fit to the data obtained, shown in Fig. 10, yielded $U=(3.2\pm0.8)\times10^4$ sec^{-1} and $c_0=0.043$. We also show in Fig. 10 the value for U_{12} determined by Bowman, Quarles, and Feldman for a 6% sample.[32] The closeness of that point to the rising portion of the curve gives us a measure of confidence in the credibility of the fit.

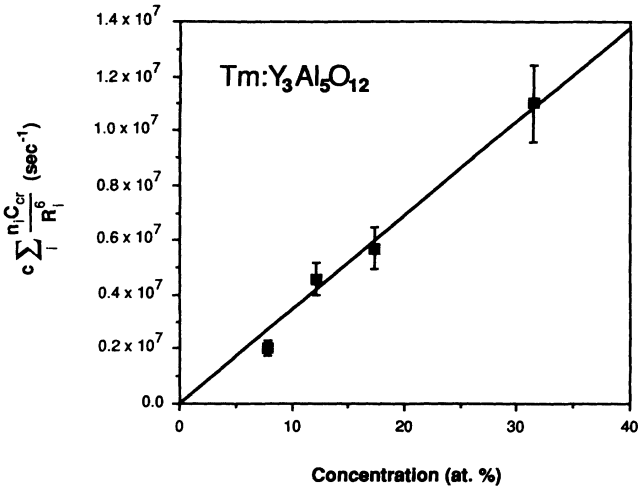

FIG. 9. Cross relaxation rate of Tm^{3+} ($^3H_4$) obtained from the initial exponential portion of the decay curve vs Tm^{3+} concentration.

In the determination of U_{13}, the quasi-steady-state N_3 was plotted against N_1 as in the case for Ho^{3+}. A quadratic dependence was found for all concentrations, as illustrated in Figs. 11(a) and 11(b). The nonexponential cross relaxation of Tm^{3+} ($^3H_4$), however, poses a problem in the application of the macroscopic rate equations. When the rate constant found from Fig. 9 was used for C_{31}, the values of U_{13} shown in Fig. 12 were found. The concentration dependence of U_{13} deduced in this manner is clearly not the same as what was found in the earlier cases. The discrepancy is not surprising, however, since for low concentrations the C_{31} adopted applies only for a small fraction of the $^3H_4$ ions. This explains the greatly

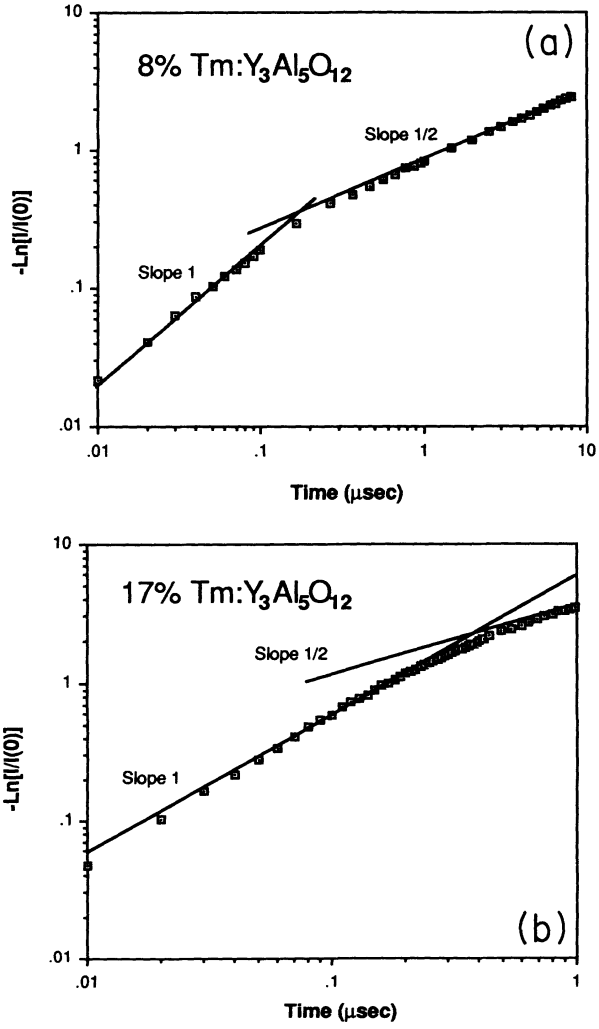

FIG. 8. Bimodal cross relaxation of Tm^{3+} ($^3H_4$) in (a) 8% $Tm:Y_3Al_5O_{12}$ and (b) 17% $Tm:Y_3Al_5O_{12}$. Plotted on the vertical axis is the negative logarithm of the fluorescence signal normalized to its initial value. Note the lengthening of the initial exponential decay portion with concentration.

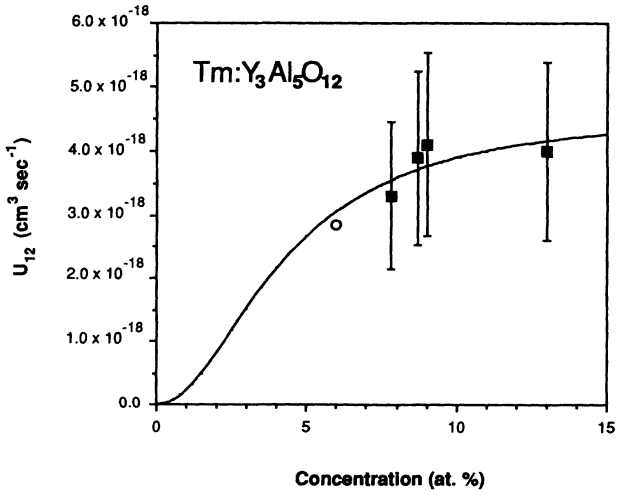

FIG. 10. Measured rate constants for up-conversion from Tm^{3+} ($^3F_4$) to Tm^{3+} ($^3H_5$) for different Tm^{3+} concentrations. The point without error bars was taken from Ref. 32 and was not used in the curve fitting.

exaggerated values of U_{13} thus determined at low concentrations. At higher concentrations our procedure is better justified. For the point with the highest concentration (34%) more than 90% of the cross relaxation of Tm^{3+} ($^3H_4$) is exponential. Therefore, we chose to determine U' by making Eq. (18) go through that single point, using the value of c_0 found from the U_{12} data. The value of U' extracted in this way was $(9\pm3)\times10^3$ sec^{-1}. The correct concentration dependence of U_{13} for $Tm:Y_3Al_5O_{12}$ is therefore given by the curve in Fig. 12 and not by the points shown (except the one for the 34% sample).

In the case of $Tm:Y_3Al_5O_{12}$ the two up-conversion transition probabilities U and U' are comparable in magnitude. One may wonder with good reason whether this situation in any way invalidates the whole analysis procedure. Once a $Tm^{3+}(^3H_4)$ ion is formed, it can cross relax within the NN pair, migrate out of that particular NN pair, or undergo radiative or multiphonon relaxation. The last possibility is negligible compared to the first two. Cross relaxation within the same NN pair clearly has no impact on our model. Migration of $^3H_4$ produces a negligible effect on our results so long as $N_e \ll N_g$. Therefore, the assumptions made in Eqs. (1)–(3) still hold, and the use of Eq. (11) is again justified.

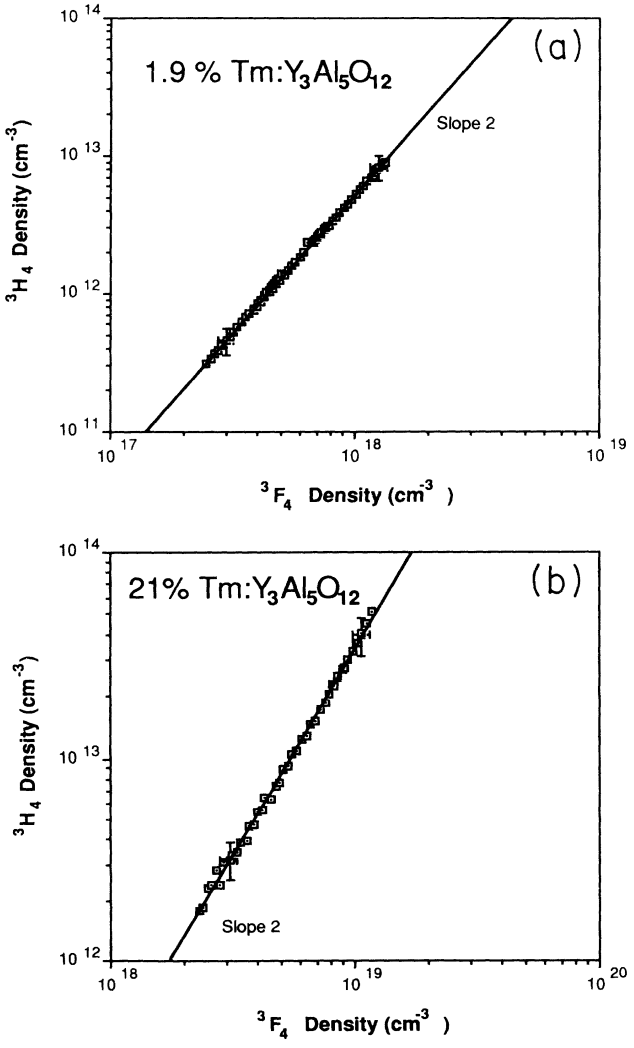

FIG. 11. Quasi-steady-state density of Tm^{3+} ($^3H_4$) plotted against that of Tm^{3+} ($^3F_4$) for (a) 1.9% $Tm:Y_3Al_5O_{12}$ and (b) 21% $Tm:Y_3Al_5O_{12}$.

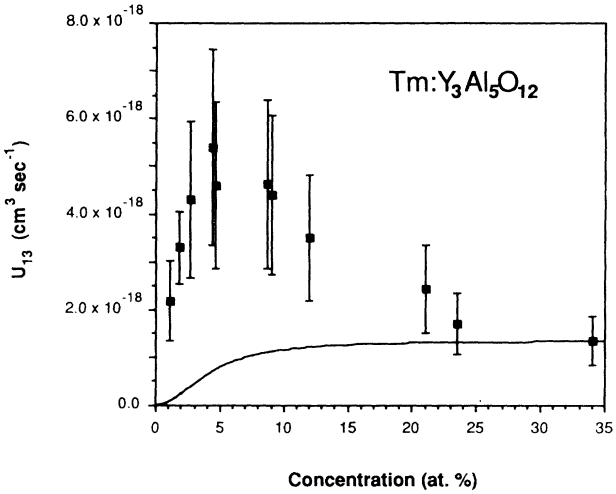

FIG. 12. "Rate constants" for up-conversion from Tm^{3+} ($^3F_4$) to Tm^{3+} ($^3H_4$) obtained by assuming that all the Tm^{3+} ($^3F_4$) ions cross relax with nearest-neighbor ground-state ions. In fact this assumption holds only for the highest concentration point. Hence, the correct concentration dependence is given by the curve drawn through the latter using the value of C_0 found from Fig. 10.

VII. DISCUSSION

In our up-conversion model we have assumed that only NN pairs can interact. The validity of this assumption can be checked by a simple calculation. For dipole-dipole interaction and uniform distribution of the second ion the total probability of transfer per unit time is given by

$$W^t(c)=c\sum_i \frac{n_i C_{\rm int}}{R_i^6}\ , \tag{20}$$

where c is the dopant concentration, $C_{\rm int}$ is the microparameter for the interaction, R_i is the distance to the $(i+1)$th closest neighbor and n_i is the corresponding coordination number. For $Y_3Al_5O_{12}$ we find that the difference between taking all terms in Eq. (20) and just the first term ($i=0$) is only a factor of 1.34.[30] Therefore, a small error is made by considering only the NN interactions. For up-conversion, however, one must also take into account the fact that the probability for a NN ion to be excited is smaller than that for a non-NN ion under migration limited conditions. Therefore, the relative importance of non-NN interactions can be significantly greater at low concentrations. For this reason, in fitting the up-conversion-rate constant vs concentration data we did not use the points for the lowest concentrations. From these considerations we would also conclude that the up-conversion transition probability determined using

Eqs. (17) and (18) might be 30% or so larger than what they should be.

We have also assumed in our model that the surrounding with which the NN pairs exchange excitation is always equilibrated. This is equivalent to saying that the diffusion length $\sqrt{2D\tau}$, where D is the metastable state diffusion coefficient and τ its lifetime in the absence of up-conversion, is much larger than the average distance between NN pairs. One may take the latter to be $(3/4\pi N_p)^{1/3}$, where N_p is as before the density of NN pairs. For Tm^{3+} ($^3F_4$) in a 10% doped crystal, for example, one calculates $\sqrt{2D\tau}=2.4\times10^{-5}$ cm (Ref. 33) and $(3/4\ \pi N_p)^{1/3}=7.7\times10^{-8}$ cm. One can therefore conclude that the metastable Tm^{3+} ions are indeed uniformly distributed (except where the ions have nearest neighbors when up-conversion is migration limited). There is no available data on the diffusion coefficient for the Ho^{3+} ($^5I_7$) metastable state. But from the numbers for Tm^{3+} ($^3F_4$) just given, one sees that even if the diffusion coefficient were two orders of magnitude smaller, the diffusion length would still be much larger than the average distance between NN pairs for dopant concentrations of a few percent or higher. Therefore, in all likelihood, the assumption was a good one in the case of Ho^{3+} also.

To place our results in the context of existing theories on phonon assisted energy transfer, it is helpful to express all of them in terms of energy-transfer probabilities. This has already been done for all but the cross relaxation of Ho^{3+} ($^5I_5$). For the latter the energy-transfer-rate constant can be converted to transfer probability by the use of

$$W_{ij}^t(c=1)=C_{ij}N_s\ , \tag{21}$$

where W_{ij}^t is defined in Eq. (20). The probability that we seek is then just the first term in the sum divided by n_0. The probabilities for energy transfer to a single nearest-neighbor ion for all the processes studied are listed in Table I.

One can also estimate the migration probabilities for the metastable states by finding C_m through the use of Eq. (11′). The probability for a metastable ion to transfer its energy to a nearest-neighbor ion is then simply C_m/R_0^6. This probability is found to be 4.6×10^7 sec^{-1} for Ho^{3+} ($^5I_7$) and 1.9×10^7 sec^{-1} for Tm^{3+} ($^3F_4$). Note that these results depend critically on the interpretation of the characteristic distance R_c which appears in Eq. (4) because of the inverse sixth power dependence, and should therefore be regarded only as estimates. However, the values of U and U' found earlier are not affected by any such changes. Furthermore, even if the interaction for energy migration is not of a dipole-dipole nature, our results for U and U' would still be approximately correct because the concentration dependent U_{12} and U_{13} data approach their asymptotic values in all cases.

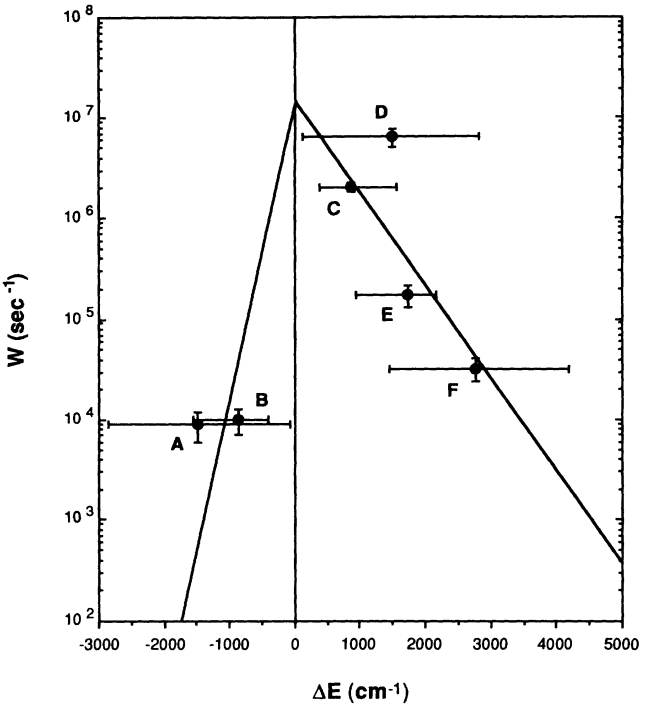

FIG. 13. The "energy-gap law" applied to the results obtained in this work for $Ho:Y_3Al_5O_{12}$ and $Tm:Y_3Al_5O_{12}$. The probability per unit time is for energy transfer between two nearest-neighbor ions ($R_0=0.37$ nm). The processes corresponding to the points labeled by the letters are given in Table I. The absolute values of the two slopes differ by $1/(kT)$.

For comparison, the migration probability inferred from earlier studies in the case of Tm^{3+} ($^3F_4$) ranged from 6×10^5 sec^{-1} (Ref. 33) and 9×10^5 sec^{-1} (Ref. 34) to 3×10^9 sec^{-1} (Ref. 35). The smallest and largest results are from grating decay measurements using two different data reduction procedures. Earlier determinations of the cross relaxation probability for Tm^{3+}($^3H_4$) can also be found in the literature. Becker *et al.* reported a microparameter of 1.8×10^{-39} $cm^6\,sec^{-1}$, which yields a probability of 0.7×10^6 sec^{-1}.[36] They did not give any details on how the determination was made. Using the decay

TABLE I. Energy-transfer probabilities for nearest-neighbor ion pairs.

Energy-transfer process	ΔE (cm^{-1})	W (sec^{-1})
A. $2Tm^{3+}$ ($^3F_4$)$\rightarrow Tm^{3+}$ ($^3H_4$)$+Tm^{3+}$ ($^3H_6$)	−1495	$(0.9\pm0.3)\times10^4$
B. $2Ho^{3+}$ ($^5I_7$)$\rightarrow Ho^{3+}$ ($^5I_5$)$+Ho^{3+}$ ($^5I_8$)	−864	$(1.0\pm0.3)\times10^4$
C. Ho^{3+} ($^5I_5$)$+Ho^{3+}$ ($^5I_8$)$\rightarrow 2Ho^{3+}$ ($^5I_7$)	864	$(2.0\pm0.2)\times10^6$
D. Tm^{3+} ($^3H_4$)$+Tm^{3+}$ ($^3H_6$)$\rightarrow 2Tm^{3+}$ ($^3F_4$)	1495	$(6.4\pm1.5)\times10^6$
E. $2Ho^{3+}$ ($^5I_7$)$\rightarrow Ho^{3+}$ ($^5I_6$)$+Ho^{3+}$ ($^5I_8$)	1723	$(1.7\pm0.4)\times10^5$
F. $2Tm^{3+}$ ($^3F_4$)$\rightarrow Tm^{3+}$($^3H_5$)$+Tm^{3+}$ ($^3H_6$)	2773	$(3.2\pm0.8)\times10^4$

curves they show in Fig. 2, we found that those for the 7×10^{19} cm^{-3} sample and the 4×10^{20} cm^{-3} sample could be fitted well to exp $(-\gamma\sqrt{t})$ and gave microparameters of 4.6×10^{-39} cm^6 sec^{-1} and 1.4×10^{-38} cm^6 sec^{-1}, respectively. The latter is almost identical to what we found from the trailing portions of our own decay curves. Armagan *et al.* reported a microparameter of 2.7×10^{-39} cm^6 sec^{-1}.[34] Our analysis of their curves yielded values ranging from 1.3×10^{-39} cm^6 sec^{-1} to 4.6×10^{-39} cm^6 sec^{-1}.

According to the Miyakawa-Dexter theory, the probability of phonon-assisted energy transfer may be expressed as[14]

$$W(\Delta E)=W(0)\exp(-\beta\Delta E)\ , \tag{22}$$

where ΔE is the difference between the transition energy of the donor and the transition energy of the acceptor, usually referred to as the energy gap. The parameter β is related to a similar one α for multiphonon relaxation by

$$\beta=\alpha-\gamma\ , \tag{23}$$

where

$$\gamma=(\hbar\omega)^{-1}\ln(1+g_b/g_a)\ . \tag{23'}$$

In the last expression $\hbar\omega$ is the energy of the phonon mode which provides the most "assistance" and g_a and g_b are electron-lattice coupling constants for the donor and acceptor transitions. The energy-transfer probabilities given in Table I are plotted against their respective energy gaps (calculated using the lowest Stark level in each manifold) in Fig. 13. The end points of the horizontal bars give the extreme values of ΔE that one finds when combinations of highest- and lowest-lying Stark levels in the initial and final states, or vice versa, are used. However, since only the thermally populated initial Stark sublevels can participate in the interaction, the horizontal bars should really be truncated to the right of the points when they are larger than ~2 kT. When a fit to Eq. (22) is made (not taking into account the spread in ΔE) for the $\Delta E>0$ points, one finds for the β parameter a value of 2.1×10^{-3} cm. The α parameter for multiphonon relaxation in $Y_3Al_5O_{12}$ is 3.1×10^{-3} cm.[37] If the assumption $g_a=g_b$ is made, one finds from Eqs. (23) and (23') that the phonons that make the greatest contributions to energy transfer in $Y_3Al_5O_{12}$ have an energy of 690 cm^{-1}. This is to be compared with the maximum phonon energy of 700 cm^{-1} for $Y_3Al_5O_{12}$ given in Ref. 37.

Equation (21) applies only when $\Delta E>0$. If the states are unsplit, from detailed balance one must have

$$W=W(0)\exp[-(\beta+1/kT)|\Delta E|]\ , \tag{24}$$

when $\Delta E<0$. The line to the left of $\Delta E=0$ in Fig. 13 was drawn using Eq. (24) and the value of β determined earlier from the $\Delta E>0$ points. It is seen to fit well our experimental data with $\Delta E<0$. The overall fit is good to about an order of magnitude, which is typical of the validity of the energy gap laws for phonon mediated nonradiative processes. One notices, however, that corresponding probabilities for opposite processes show more or less the same deviations from the best fit (i.e., B and C are both slightly below the lines, and A and D both lie high above the lines). Thus, if the probability for one of the processes is known, one may be able to estimate the probability for the opposite process with considerably better accuracy than order of magnitude with the help of the energy-gap law plot. Further experiments to substantiate this correlation in $Y_3Al_5O_{12}$ as well as other crystals will be of interest.

ACKNOWLEDGMENTS

We wish to thank X. B. Jiang for his help in the growth of the crystals used in this experiment. This work was supported in part by the Office of Naval Research.

[1]J. C. Wright, in *Radiationless Processes in Molecules and Condensed Phases,* edited by F. K. Fong (Springer-Verlag, Berlin, 1976).

[2]B. M. Antipenko, S. P. Voronin, and T. A. Privalova, Sov. Phys. Tech. Phys. **32**, 208 (1987).

[3]F. Tong, W. P. Risk, R. M. Macfarlane, and W. Lenth, Electron. Lett. **25**, 1389 (1989).

[4]T. Hebert, R. Wannemcher, W. Lenth, and R. M. Macfarlane, Appl. Phys. Lett. **57**, 1727 (1990).

[5]A. J. Silversmith, J. Opt. Soc. Am. A **3**, P128 (1986).

[6]R. M. Macfarlane, F. Tong, A. J. Silversmith, and W. Lenth, Appl. Phys. Lett. **52**, 1300 (1988).

[7]T. Hebert, R. Wannemacher, W. Lenth, and R. M. Macfarlane, Appl. Phys. Lett. **60**, 2592 (1992).

[8]B. P. Scott, F. Zhao, R. S. F. Chang, and N. Djeu, Opt. Lett. **18**, 113 (1993).

[9]T. Y. Fan, G. Huber, R. L. Byer, and P. Mitzscherlich, IEEE J. Quantum Electron. **QE-24**, 924 (1988).

[10]S. R. Bowman, M. J. Winings, R. C. Y. Auyeung, J. E. Tucker, S. K. Searles, and B. J. Feldman, IEEE J. Quantum Electron. **QE-27**, 2142 (1991).

[11]M. A. Noginov, H. P. Jenssen, and A. Cassanho, in *Advanced Solid State Lasers,* Vol. 15 of OSA Proceedings Series, edited by A. A. Pinto and T. Y. Fan (Optical Society of America, Washington, D.C., 1993), p. 376.

[12]L. K. Smith, S. A. Payne, J. B. Tassano, L. D. DeLoach, W. L. Kway, and W. F. Krupke, in *Advanced Solid State Lasers* (Ref. 11), 1993, p. 381.

[13]D. L. Dexter, J. Chem. Phys. **21**, 836 (1953).

[14]T. Miyakawa and D. L. Dexter, Phys. Rev. B **1**, 2961 (1970).

[15]N. Yamada, S. Shinoya, and T. Kushida, J. Phys. Soc. Jpn. **32**, 1577 (1972).

[16]V. P. Sakun, Sov. Phys. Solid State **14**, 1906 (1973).

[17]Y. K. Voronko, T. G. Mamedov, V. V. Osiko, A. M. Prokhorov, V. P. Sakun, and I. A. Shcherbakov, Sov. Phys. JETP **44**, 251 (1976).

[18]A. A. Kamisnkii, *Laser Crystals* (Springer-Verlag, Berlin, 1981).

[19]I. A. Bondar, A. I. Burshtein, A. V. Krutikov, L. P. Mezentseva, V. V. Osiko, V. P. Sakun, V. A. Smirnov, and I. A. Shcherbakov, Sov. Phys. JETP **54**, 45 (1981).

[20]V. V. Osiko, Y. K. Voronko, and A. A. Sobol, in *Growth and Defect Structures,* edited by H. C. Freyhardt (Springer-Verlag, Berlin, 1984).

[21]M. A. Gilleo and S. Geller, Phys. Rev. **110**, 73 (1958).

[22]R. S. F. Chang, S. Sengupta, G. J. Dixon, L. B. Shaw, and N.

Djeu, Proc. Soc. Photo-Opt. Instrum. Eng. **1104**, 244 (1989).
[23]F. K. Fong and D. J. Diestler, J. Chem. Phys. **56**, 2875 (1972).
[24]P. P. F'elfilov and V. V. Ovsyankin, Appl. Opt. **6**, 1828 (1967).
[25]B. R. Judd, Phys. Rev. **127**, 750 (1962).
[26]G. S. Ofelt, J. Chem. Phys. **37**, 511 (1992).
[27]A. A. Kaminskii and B. M. Antipenko, *Multilevel Operating Schemes of Crystalline Lasers* (Nauka, Moscow, 1989).
[28]Note that the results presented here differ from the preliminary data reported earlier by us at conferences.
[29]J. A. Caird, L. G. DeShazer, and J. Nella, IEEE J. Quantum Electron. **QE-11**, 874 (1975).
[30]K. B. Sherstnev, Opt. Spectrosc. **33**, 156 (1972).
[31]R. Clausen, U. Recksiek, and G. Huber, in *Digest of Conference on Lasers and Electro-Optics* (Optical Society of America, Washington, D.C., 1990), paper JWB2.
[32]S. R. Bowman, G. J. Quarles, and B. J. Feldman, in *Advanced Solid State Lasers,* Vol. 13 of OSA Proceedings Series, edited by A. A. Pinto and T. Y. Fan (Optical Society of America, Washington, D.C., 1992), p. 169.
[33]V. A. French, R. R. Petrin, R. C. Powell, and M. Kokta, Phys. Rev. B **46**, 8018 (1992).
[34]G. Armagan, A. M. Bouncristiani, and B. DiBartolo, Opt. Mater. **1**, 11 (1992).
[35]V. A. French and R. C. Powell, Opt. Lett. **16**, 666 (1991).
[36]T. Becker, R. Clausen, G. Huber, E. W. Duczynski, and P. Mitzscherlich, in *Tunable Solid State Lasers,* Vol. 5 of OSA Proceedings Series, edited by M. L. Shand and H. P. Jenssen (Optical Society of America, Washington, D.C., 1989), p. 150.
[37]J. M. F. van Dijk and M. F. H. Schuurmans, J. Chem. Phys. **78**, 5317 (1983).